



## CoMFA-based comparison of two models of binding site on adenosine A<sub>1</sub> receptor

Irini Doytchinova

*Department of Chemistry, Faculty of Pharmacy, Medical University Sofia, 1000 Sofia, Bulgaria (Tel.: +359 2 59 22 01; Fax +359 2 987 98 74; E-mail: irini@mbbox.pharmfac.acad.bg)*

Received 17 November 1999; Accepted 17 May 2000

**Key words:** adenosine agonists, adenosine antagonists, CoMFA, 8-substituted xanthines, N6-substituted adenosines, 3D-QSAR

### Summary

A set of 32 N6-substituted adenosines and 22 8-substituted xanthines with affinity for adenosine A<sub>1</sub> receptors was subjected to three-dimensional quantitative structure-affinity relationship analysis using comparative molecular field analysis (CoMFA). The aim was to compare two modes of binding to the receptor – ‘N6-C8’ and ‘N6-N7’. Good models with high predictive power and stability were obtained. A comparison of these models gives the following results: (a) Inclusion of both steric and electrostatic fields in CoMFA generates better predictive models compared to models based on steric or electrostatic fields alone. (b) The ‘N6-N7’ CoMFA models are slightly better than the ‘N6-C8’ ones. (c) Steric restriction exists around the N6-H in the ‘N6-N7’ steric field map, which is absent in the ‘N6-C8’ steric field map. This report demonstrates that the ‘N6-N7’ mode of binding is a further development of the ‘N6-C8’ model with a slightly better predictive ability and more accurate steric and electrostatic overlaps between agonists and antagonists.

### Introduction

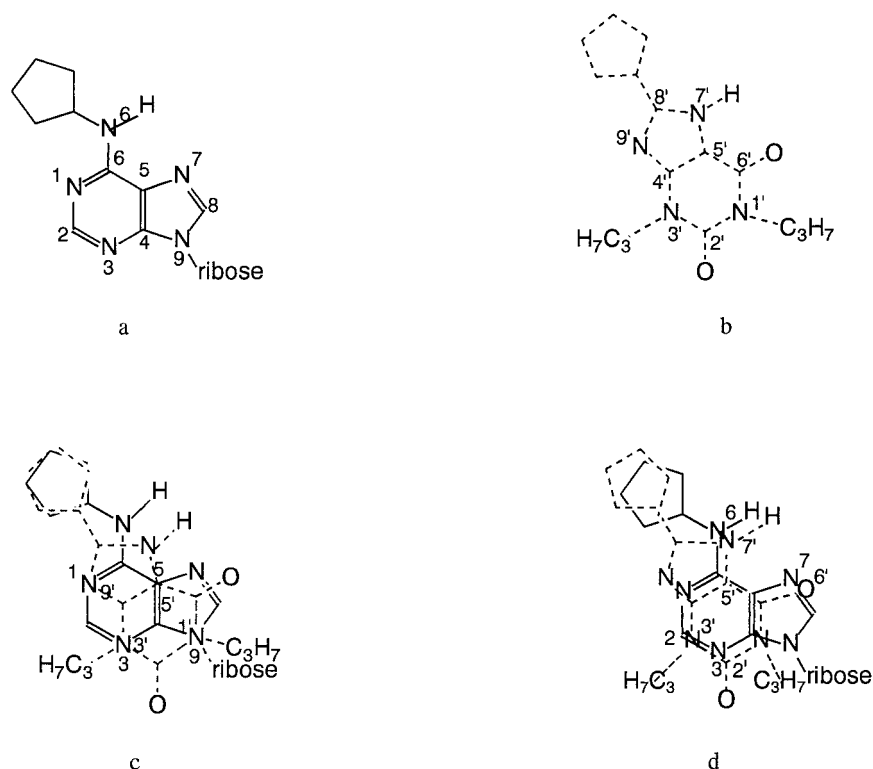
Adenosine receptors (AR) are subdivided into four subtypes A<sub>1</sub>, A<sub>2a</sub>, A<sub>2b</sub> and A<sub>3</sub>, that can be distinguished pharmacologically, based on the rank order of potency of agonists and antagonists. These receptors belong to the superfamily of G protein-coupled receptors and contain seven transmembrane domains ( $\alpha$ -helices), interconnecting loops, an extracellular terminal amino residue, and a cytoplasmic terminal carboxylate residue [1]. The intracellular enzyme adenylate cyclase is inhibited by the A<sub>1</sub> and A<sub>3</sub> subtypes of the receptor (termed G<sub>i</sub>) and stimulated by the A<sub>2a</sub> and A<sub>2b</sub> subtypes (termed G<sub>s</sub>).

It is generally assumed that AR agonists and antagonists bind to the same receptor site. Models have been developed for the binding mode of adenosine derivatives with respect to xanthines at A<sub>1</sub> AR. These models are based on steric, electrostatic and hydrophobic comparisons [2, 3]. Agreement appears to exist that the so-called ‘N6-C8’ model is the preferred mode

of ligand binding to the receptor (Figure 1c) [3, 4]. In this model N1, N3 and N9 of adenosine (Figure 1a) overlay with N9, N3 and N1 of xanthine (Figure 1b, labelled by ‘), respectively. This superposition places the acidic hydrogen atoms of both ligands in the same proximity; thus the N7-H of xanthine is close to one of the C6 amino hydrogen atoms of adenosine. It is generally known that the acidic NH groups in the agonist and antagonist ligands are necessary for high adenosine A<sub>1</sub> receptor affinity.

Recently a modification was proposed of the ‘N6-C8’ model, named ‘N6-N7’, with improved steric and electrostatic fit (Figure 1d) [5]. In this new mode of binding the positions of atoms C2, N3, N6 and N7 of the adenine moiety coincide with N3, C2, N7 and O6 of the xanthine ring (labelled by ‘), respectively. Despite the steric and electrostatic resemblance between the ‘N6-C8’ and ‘N6-N7’ models, there is no one atom pair common to the two models.

In order to assess the mode of binding of different ligands with affinity to the same biomacromolecule,



**Figure 1.** A<sub>1</sub> AR ligands and models for the binding mode on A<sub>1</sub> adenosine receptors. (a) A<sub>1</sub> agonist N6-cyclopentyladenosine (CPA). (b) A<sub>1</sub> antagonist 1,3-dipropyl-8-cyclopentylxanthine (DPCPX). (c) Model 'N6-C8': the atoms N1, N3, C5 and N9 of the adenine moiety coincide with N9', N3', C5' and N1' of the xanthine ring. (d) Model 'N6-N7': the atoms C2, N3, N6 and N7 of the adenine moiety coincide with N3', C2', N7' and O6' of the xanthine ring.

the CoMFA method [6–8] compares the steric, electrostatic, and hydrophobic fields around the aligned ligands. The aim of the present study is to apply the CoMFA technique to 32 adenosines and 22 xanthines with affinity to adenosine A<sub>1</sub> receptors and compare the predictive power of the two alignment models, 'N6-C8' and 'N6-N7'.

## Computational methods

### Biological data

Tables 1 and 2 list the structures with the observed and calculated affinity values of the adenosines and xanthines forming the training set used to derive the CoMFA models. The A<sub>1</sub> adenosine receptor binding affinity values of these compounds were taken from the literature and expressed as pK<sub>i obsd</sub>, where K<sub>i</sub> values were generated from the inhibition of binding of [<sup>3</sup>H]CHA or [<sup>3</sup>H]R-PIA to A<sub>1</sub> adenosine receptors in rat cerebral cortical membranes [9–13]. The series of

adenosines consists of N6-substituted analogues. As the alignment of agonists and antagonists is in the purine domain, the ribose moiety does not affect the mode of alignment but only complicates the CoMFA calculations. To avoid this complication the ribose ring was replaced by a methyl group [14]. The series of xanthines includes 8-substituted 1,3-dimethyl and 1,3-dipropyl derivatives. Compounds with high, moderate and low affinities were included in the present study. The range in affinity is slightly less than 5 log units.

### 3D molecular databases

All molecular modelling and CoMFA calculations were performed using the modeling package Chem-X (version July 1998) [15]. The main rings of **R-PIA** and **DPCPX**, optimized previously in our work [5], were used to build the respective adenosines and xanthines. Conformational analysis was performed of the bond connecting the main ring and the N6/C8 substituent. Global minimum conformers were chosen for the adenosines. Local minimum conformers with C8 sub-

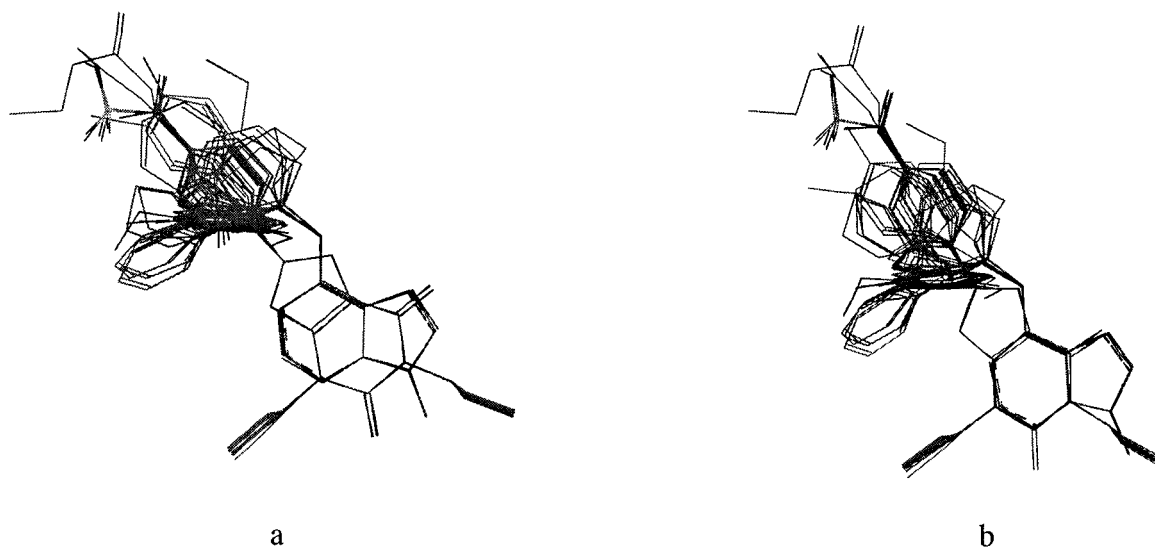


Figure 2. Alignment of the structures according to the 'N6-C8' (a) and 'N6-N7' (b) rules.

stituents oriented opposite to N7 were chosen for the xanthines. The structures were geometry optimized using the MM2 force field with a 0.0001 energy gradient convergence criterion [16]. The final optimization was performed with a semiempirical molecular orbital method by MOPAC (ChemQM module of Chem-X) applying the AM1 Hamiltonian [17]. The output option included partial atomic charges which were used in CoMFA. After optimization the structures were compiled in a 3D database.

#### Alignment rules

The most crucial variable in CoMFA is the alignment of the molecules. Four 3D queries were defined, called 'ado', 'xant', 'N6-C8' and 'N6-N7'. The first query was used for the alignment of the molecules of adenosine derivatives only. It consisted of the adenine moiety. The xanthine ring formed the 'xant' query which was used for the alignment of the xanthine analogues. The 'N6-C8' query included the atoms N1, N3, C5, N6, H6, N7 and N9 from the molecule of adenosine. The O6-atom from the molecule of xanthine was accepted as equivalent to N7. The compounds were superimposed to the query by a least-squares algorithm. The alignment of the molecules according to the 'N6-C8' rule is presented in Figure 2a. The 'N6-N7' query includes the atoms N1, C2, N3, C4, C5, C6, N6 and N7 from adenosine. C4 and C2 from the xanthines were accepted as equivalent to N1 and N3 from adenosine, N3 and N1 as equivalent to C2 and C4, and

O6 as equivalent to N7. The 'N6-N7' alignment rule is presented in Figure 2b. As defined the 3D queries were used in the 3D search on the whole of the 3D database previously compiled. To match all the atoms in the query to structures in the database the {Fit All Atoms} option was used. The search was limited to the conformers included in the database.

#### CoMFA method

The comparative molecular field analysis (CoMFA) was performed using the SAR option of Chem-X. The partial atomic charges used in CoMFA were computed using the AM1 semiempirical method available in the MOPAC program. To obtain the steric and electrostatic probe-ligand interaction energies (eV/mol), van der Waals volume and potential maps were generated for each of the structures in the database. The grid size was set to 1.0 point per Angstrom. The electrostatic potential was defined as the interaction energy of a point positive unit charge with the atoms of the structure.

The QSAR table was built with the compounds as row entries and two column entries:  $pK_i$  values (dependent variables) and the steric and electrostatic field potential values (independent variables). Partial least-squares (PLS) methodology [18] was used to analyse the relationship between the independent variables and the  $pK_i$  values. In a single-pass PLS calculation all the structures in the input table were used to generate the components. The degree of variance in the data which

is to be explained by the PLS components can be specified as the target variance. Its value was accepted to be the default value of 80%.

The cross-validation PLS calculation was performed by a leave-one-out procedure. The models were estimated on the basis of the non-cross-validated  $r^2$ , the cross-validated  $r^2$  (expressed as  $q^2$ ), and the standard error of prediction,  $e_{\text{PRESS}}$ .  $e_{\text{PRESS}}$  was calculated by the equation  $e_{\text{PRESS}} = (\text{PRESS}/p - 1)^{1/2}$ , where  $\text{PRESS} = \sum (pK_{\text{i pred}} - pK_{\text{i obsd}})^2$  and  $p$  is the total number of structures omitted.

In order to assess the stability of the models a number of samples was created. Sets with reduced numbers of compounds with one of the group omitted were developed as explained by Wold [19]. The omitted data were used as a test set, and differences between observed and predicted affinities were calculated for the test set. The predictive capability of the models was assessed by  $q^2$  and  $e_{\text{PRESS}}$ . The number of samples was varied between five and nine, and the number of compounds omitted was varied from nine to five, respectively. The mean value of  $q^2$  from this non-leave-one-out cross-validation procedure was compared both to the  $q^2$  from the leave-one-out procedure and to the non-cross-validated  $r^2$ . The closeness of values is an indicator for the stability of the obtained models [19].

The steric and electrostatic features of the final CoMFA models were displayed as contour plots of the PLS regression coefficients at each CoMFA region grid point using the WLS option of Chem-X. The 'positive' steric contour was coloured black and the 'negative' steric contour was colored grey. The electrostatic contributions were displayed in a similar fashion with black-coloured positive contours (ligand interaction with the positive probe in these regions enhances affinity) and grey-colored negative contours (ligand interaction with the positive probe in these regions lowers affinity).

## Results

Every QSAR investigation is based on an assumption of homogeneity. This implies similarity in the biological mode of action of all the investigated compounds, which in turn corresponds to having some limits on structural variability and diversity. In order to achieve a satisfactory homogeneity in the series of adenosines as well as the xanthine analogs, preliminary CoMFA on each series were performed.

### CoMFA on adenosines

The single-pass PLS calculation on the training set of 32 adenosines accounting for the CoMFA steric and electrostatic fields gave an optimum principal component number of three. The non-cross-validated  $r^2$  was 0.7430. In the cross-validation PLS calculation the cross-validated  $q^2$  was negative (Table 3, model 1). This model was of low quality and could not predict much better than chance since  $q^2$  is negative. The score plot of the first two principal components shows that the compounds **1**, **2**, **3**, **4**, **15**, **16** and **17** deviate from the other adenosines (plot is available as Supporting Information). Compounds **1**, **2** and **3** possess bulky substituents at N6, but compounds **15**, **16** and **17** are the only ones in the set having the hydrophobic cycloalkylphenyl moiety two carbons away from N6. Compound **4** has the lowest affinity in the set of adenosines. The exclusion of these compounds from the data set generated model 2 which was substantially better with two significant components and  $r^2 = 0.9509$ ,  $q^2 = 0.6960$ . This marked improvement indicated that the data set was now homogeneous and could be properly modelled. Thus, the final set of adenosines consisted of 25 compounds. The steric-field model produces better prediction results than the electrostatic-field one, as evident from models 3 and 4 (Table 3).

### CoMFA on xanthines

Two principal components explained more than 80% of total variance of the CoMFA model on xanthines (Table 4, model 5). The score plot distinguished as outliers the compounds **42** and **43** (plot is available as Supporting Information). They both have the lowest  $A_1$  affinities in the set of 1,3-dipropyl-8-substituted xanthines. Evidently, the  $A_1$  receptor cannot accommodate such polar moieties as 8-piperidinyl and 8-pyrazinyl. The model without these compounds had good predictive power (Table 4, model 6). Thus, 20 compounds formed the final set of xanthines. Comparison of models 7 and 8 indicated that the electrostatic requirements are more important than the steric ones.

### 'N6-C8' CoMFA model

A CoMFA model derived from the affinities of the compounds from the final sets of adenosines and xanthines was obtained using the 'N6-C8' alignment rule discussed in the Computational methods section. Table 5 contains the statistics of the 'N6-C8' CoMFA

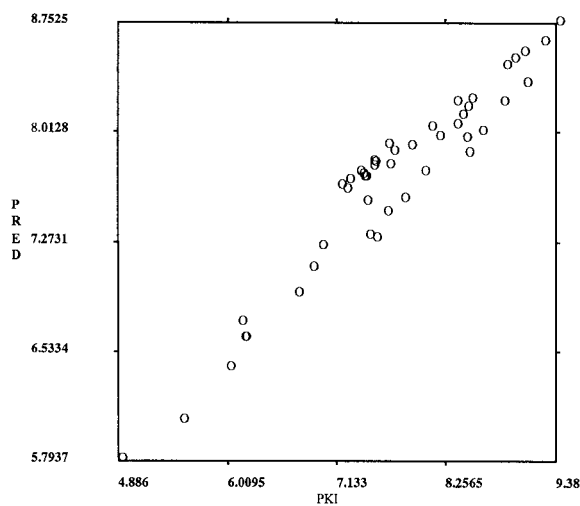


Figure 3. Predicted (PRED) versus observed  $pK_i$  values according to the 'N6-C8' CoMFA model (model 9, Table 5).

model. Two components explained more than 80% of total variance. Model 9 had good predictive power ( $q^2 = 0.7253$ ). The electrostatic contribution term was greater than the steric one (models 10 and 11). Observed and calculated  $pK_i$  values are listed in Table 1 and plotted in Figure 3. Actually, the predicted values for the  $A_1$  AR affinity are referring to the corresponding 9-methyl adenines. The close values of the observed and predicted affinities could be considered as evidence for the assumption that the AR affinity is determined by the purine domain of the ligands, but the intrinsic activity by the ribose residuals [20].

The stability of model 9 was investigated by varying the number of compounds omitted as described in Computational methods. The  $q^2$  values for the 'N6-C8' alignment rule vary from 0.6917 to 0.7645 with a mean value of 0.7225 (Table 6). This  $q^2$  mean value is nearly the same as the  $q^2$  from the leave-one-out cross-validation procedure (0.7225 and 0.7253, respectively). The cross-validated  $q^2$  values are closer to  $r^2$  from the non-cross-validated analysis (0.8251), illustrating the stability of the obtained model.

In order to visualize the information content of the derived 3D-QSAR model, CoMFA coefficient maps were generated. As is known, these maps cannot be considered as a receptor model, because structural modulation does not usually concern the active sites of molecules. They can only delineate the areas of the lattice points characterized by variance of the steric and electrostatic properties of the ligands.

Figure 4 shows the CoMFA steric and electrostatic contour map using compound **R-PIA** as a reference

Table 3. Statistics of the CoMFA on adenosines

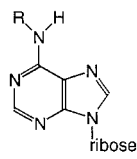
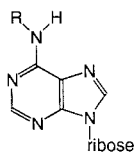

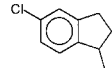

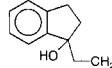
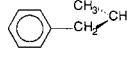
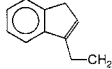
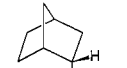
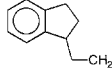
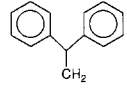
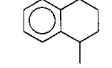
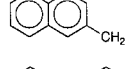
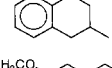
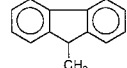
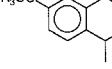
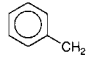
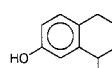

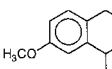
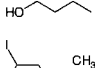
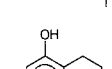
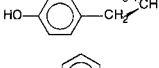
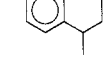

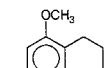
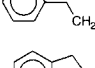
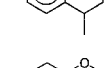
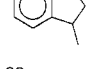
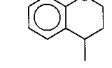
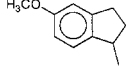
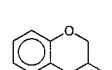
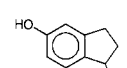
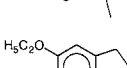
CoMFA model	<i>n</i>	PC <sup>a</sup>	$q^2$	$e_{PRESS}$	$r^2$
Model 1					
steric + electrostatic	32	3	-3.1416	1.3580	0.7430
Model 2					
steric + electrostatic	25 <sup>b</sup>	2	0.6960	0.3822	0.9509
Model 3					
only steric	25 <sup>b</sup>	2	0.8092	0.3027	0.8940
Model 4					
only electrostatic	25 <sup>b</sup>	2	0.6508	0.4095	0.9233

<sup>a</sup>Number of principal components explaining more than 80% of total variance; <sup>b</sup>without compounds **1**, **2**, **3**, **4**, **15**, **16** and **17**.

structure. The black and grey polyhedra describe regions of space whose occupancy by the ligands respectively increase or decrease affinity for the adenosine  $A_1$  receptor. The black contours around the main aromatic ring and the N6-substituent are in full agreement with the generally accepted pharmacophore model for  $A_1$ -AR ligands including the central heteroatomic domain (purine or xanthine) and a lipophilic domain near to N6 [20]. The grey contour surrounding the molecule of **R-PIA** is related to the presence of a steric restriction in the receptor cavity delimiting the volume accessible to the ligands. Out of this volume are situated the  $SO_3H$  and  $COOH$  groups from the C8 substituents. It is interesting to mention that the 'unfavourable' contour is interrupted near C2-H. This means that substituents at these positions may exist. Although there are no examples in the examined set, there is evidence that small lipophilic substituents such as Cl, F, I at position 2 enhance the  $A_1$  affinity [21–23]. The contours around the  $CH_3$  group at position 9 should be ignored because in reality a ribose moiety exists there.

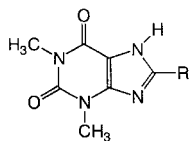

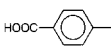
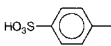

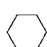
The electrostatic contour map is represented by black and grey polyhedra describing regions where a high electron density within the ligand structure increases or decreases, respectively, the affinity. The black contours surrounding the main aromatic ring and the substituent at N6 show that negative potentials in such positions increase the  $A_1$ -AR affinity. The grey polyhedra around N6-H, C2-H and C8-H suggest that positive potentials in these regions enhance the potency. As in the steric map, the contour around the methyl group at position 9 should be ignored.

Table 1. A<sub>1</sub>-AR affinities of N6-substituted adenosines (pK<sub>i</sub> obsd) with CoMFA predictions according to the 'N6-C8' model (pK<sub>i</sub> pred 'N6-C8') and the 'N6-N7' model (pK<sub>i</sub> pred 'N6-N7')

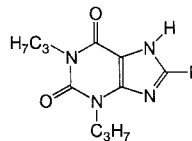

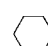
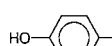
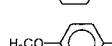
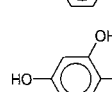
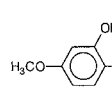
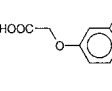
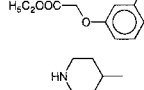
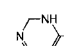
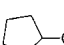
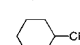

									
compd	R	pK <sub>i</sub> obsd a	pK <sub>i</sub> pred 'N6-C8' b	pK <sub>i</sub> pred 'N6-N7' c	compd	R	pK <sub>i</sub> obsd a	pK <sub>i</sub> pred 'N6-C8' b	pK <sub>i</sub> pred 'N6-N7' c
CPA		9.23	8.61	8.73	14		7.39	7.69	7.54
CHA		8.85	8.45	8.47	15		7.17	-	-
R-PIA		8.93	8.50	8.63	16		7.49	-	-
S-ENBA		9.38	8.75	8.84	17		8.29	-	-
1		8.17	-	-	18		7.47	7.77	7.73
2		7.62	-	-	19		8.08	8.03	8.05
3		8.28	-	-	20		7.15	7.65	7.50
4		6.92	-	-	21		7.40	7.70	7.72
5		8.49	8.22	8.29	22		7.64	7.78	7.85
6		8.15	7.97	8.02	23		7.69	7.87	7.79
7		9.03	8.54	8.67	24		7.63	7.91	7.83
8		8.34	8.20	8.28	25		7.20	7.61	7.57
9		8.39	8.12	8.14	26		7.87	7.90	7.97
10		7.34	7.73	7.62	27		7.50	7.80	7.80
11		7.23	7.68	7.51	28		8.44	8.17	8.26
12		7.37	7.71	7.59					
13		7.48	7.80	7.66					

<sup>a</sup>pK<sub>i</sub> is -logK<sub>i</sub>, where K<sub>i</sub> values are generated from the inhibition of binding of [<sup>3</sup>H]CHA or [<sup>3</sup>H]R-PIA to A<sub>1</sub> adenosine receptors in rat cerebral cortical membranes. Results for compounds CPA, CHA, R-PIA, S-ENBA, 1-5 are from Reference 9; those for 6-9 are from Reference 10; those for 10-28 are from Reference 11.

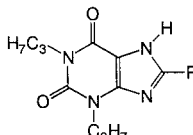

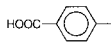
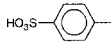
Table 2. A<sub>1</sub>-AR affinities of C8-substituted xanthines (pK<sub>i</sub> obsd) with CoMFA predictions according to the 'N6-C8' model (pK<sub>i</sub> pred 'N6-C8') and the 'N6-N7' model (pK<sub>i</sub> pred 'N6-N7')

				
compd	R	pK <sub>i</sub> obsd <sup>a</sup>	pK <sub>i</sub> pred 'N6-C8' <sup>b</sup>	pK <sub>i</sub> pred 'N6-N7' <sup>c</sup>
theophylline	H	4.89	5.79	5.72
8-phenyl		6.12	6.72	6.74
theophylline				
29		5.52	6.06	6.00
30		6.00	6.41	6.00
31		7.62	7.46	7.47
32		6.96	7.23	7.25

				
compd	R	pK <sub>i</sub> obsd <sup>a</sup>	pK <sub>i</sub> pred 'N6-C8' <sup>b</sup>	pK <sub>i</sub> pred 'N6-N7' <sup>c</sup>
DPCPX		9.05	8.33	8.33
35		8.82	8.20	8.24
36		8.46	7.86	7.91
37		8.43	7.96	7.92
38		8.60	8.01	8.14
39		8.34	8.05	8.12
40		7.43	7.30	7.34
41		7.51	7.28	7.33
42		6.21	-	-
43		6.22	-	-
44		7.80	7.55	7.53
45		7.41	7.53	7.46

				
compd	R	pK <sub>i</sub> obsd <sup>a</sup>	pK <sub>i</sub> pred 'N6-C8' <sup>b</sup>	pK <sub>i</sub> pred 'N6-N7' <sup>c</sup>
1,3-dipropyl	H	6.15	6.61	6.57
xanthine				
1,3-dipropyl		8.00	7.73	7.77
8-phenyl				
xanthine				
33		6.70	6.91	6.86
34		6.85	7.08	7.08

<sup>a</sup>pK<sub>i</sub> is  $-\log K_i$ , where K<sub>i</sub> values are generated from the inhibition of binding of [<sup>3</sup>H]CHA or [<sup>3</sup>H]R-PIA to A<sub>1</sub> adenosine receptors in rat cerebral cortical membranes. Results for theophylline, 8-phenyltheophylline, 1,3-dipropylxanthine, 1,3-dipropyl-8-phenylxanthine, DPCPX and compounds 29–35 are from Reference 12; those for 36–45 are from Reference 13.

#### 'N6-N7' CoMFA model

The CoMFA model obtained according to the 'N6-N7' alignment rule yielded good cross-validated and non-cross-validated results ( $q^2 = 0.7828$ ,  $r^2 = 0.8653$ ) with the optimal number of components found to be two (Table 7, model 12). In contrast to the 'N6-C8' CoMFA model, in the 'N6-N7' CoMFA model the steric contribution term was slightly greater than the electrostatic one (Table 7, models 13 and 14). Ob-

served and calculated according to the 'N6-N7' model pK<sub>i</sub> values are listed in Table 1 and plotted in Figure 5.

Varying the number of compounds omitted, the  $q^2$  values of model 12 vary from 0.7009 to 0.7797 with a mean of 0.7358 (Table 6). This  $q^2$  mean value is close to the  $q^2$  from the leave-one-out procedure and to the non-cross-validated  $r^2$  (0.7358, 0.7828 and 0.8653, respectively), demonstrating the stability of model 12.

The 'N6-N7' CoMFA steric and electrostatic fields are shown as coefficient maps in Figure 6. Both maps

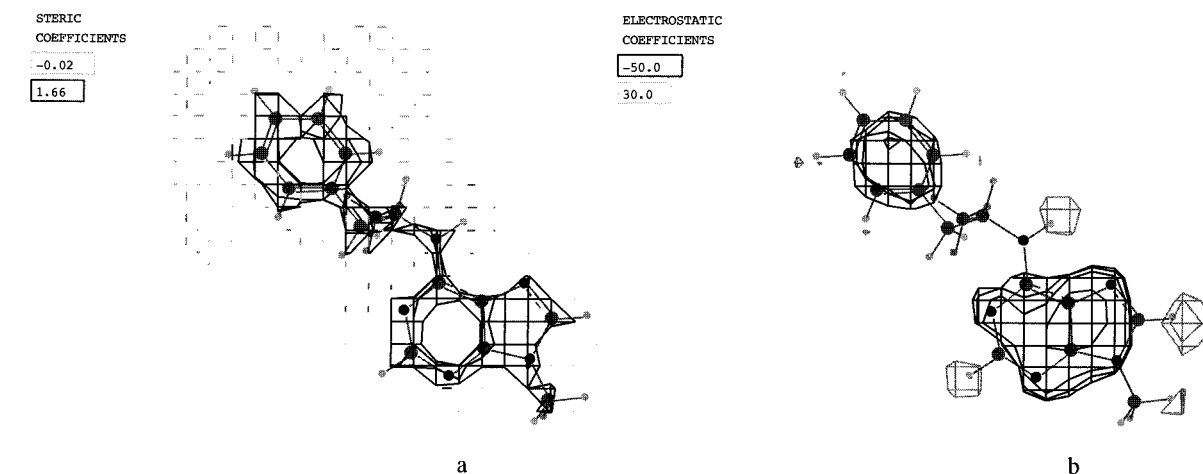


Figure 4. 'N6-C8' CoMFA maps using **R-PIA**. (a) Steric coefficient map: the black and grey polyhedra describe regions of space whose occupancy by the ligands respectively increases or decreases affinity for the adenosine A<sub>1</sub> receptor (model 10, Table 5). (b) Electrostatic map: the black and grey polyhedra describe regions where a high electron density within the ligand structure increases or decreases, respectively, the affinity for the adenosine A<sub>1</sub> receptor (model 11, Table 5).

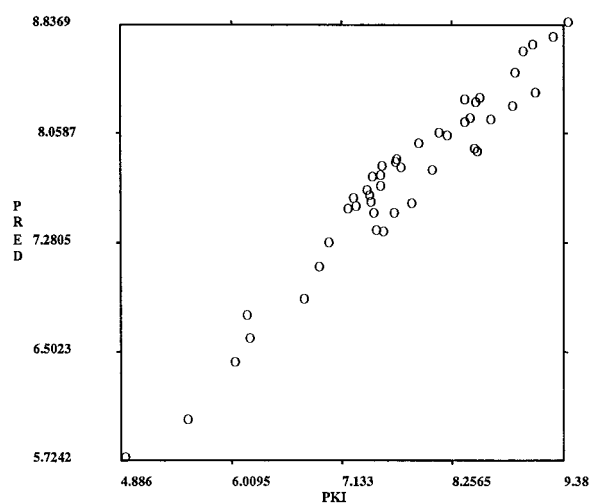


Figure 5. Predicted (PRED) versus observed  $pK_i$  values according to the 'N6-N7' CoMFA model (model 12, Table 7).

Table 4. Statistics of the CoMFA on xanthines

CoMFA model	<i>n</i>	PC <sup>a</sup>	$q^2$	$e_{PRESS}$	$r^2$
Model 5					
steric + electrostatic	22	2	0.3669	0.9186	0.8667
Model 6					
steric + electrostatic	20 <sup>b</sup>	2	0.7295	0.6051	0.9193
Model 7					
only steric	20 <sup>b</sup>	2	0.7275	0.6073	0.8671
Model 8					
only electrostatic	20 <sup>b</sup>	2	0.8275	0.6341	0.9399

<sup>a</sup>Number of principal components explaining more than 80% of total variance; <sup>b</sup>without compounds **42** and **43**.

Table 5. Statistics of the 'N6-C8' CoMFA model

CoMFA model	<i>n</i>	PC <sup>a</sup>	$q^2$	$e_{PRESS}$	$r^2$
Model 9					
steric + electrostatic	45	2	0.7253	0.5120	0.8251
Model 10					
steric + electrostatic	45	3	0.5014	0.6898	0.6452
Model 11					
only steric	45	3	0.5880	0.6270	0.6371

<sup>a</sup>Number of principal components explaining more than 80% of total variance.

are very similar to the corresponding coefficient maps, constructed according to the 'N6-C8' model (Figure 4). The main difference between the steric field maps is the presence of a steric restriction around the N6-H in the 'N6-N7' map. There is not a substantial difference between the electrostatic field maps created according to the two modes of binding.

## Discussion

The comparison of the CoMFA models generated according to the two alignment rules, 'N6-C8' and 'N6-N7', leads to three important conclusions.

(a) Inclusion of both steric and electrostatic fields in CoMFA generates models with better predictive quality than those based on steric or electrostatic fields alone (Tables 5 and 7). This means that the affinity



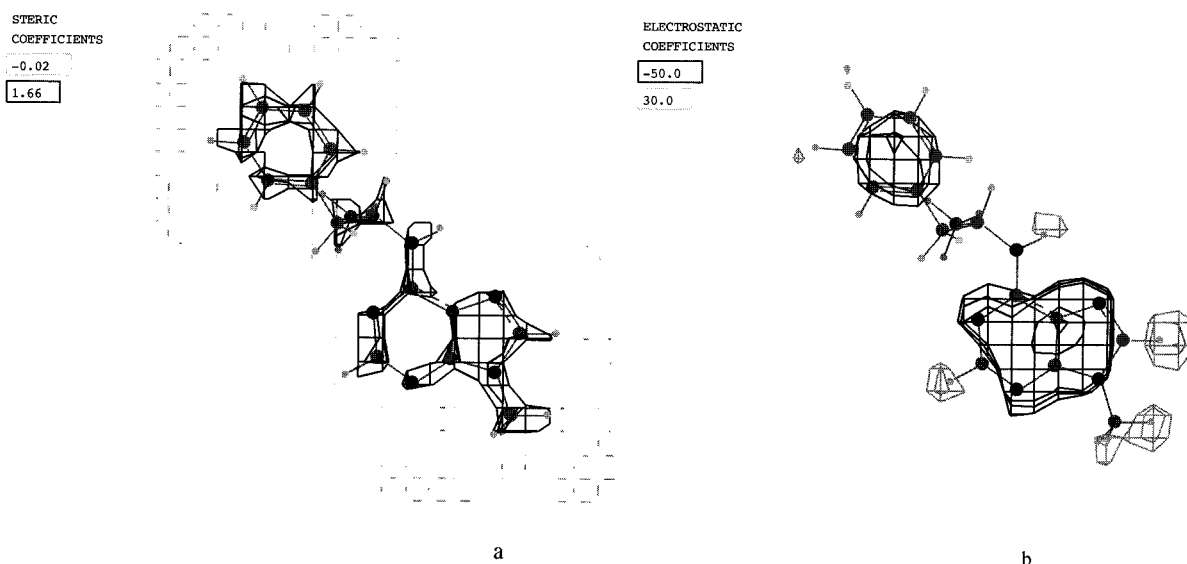


Figure 6. 'N6-N7' CoMFA maps using **R-PIA**. (a) Steric coefficient map: the black and grey polyhedra describe regions of space whose occupancy by the ligands respectively increases or decreases affinity for the adenosine A<sub>1</sub> receptor (model 13, Table 7). (b) Electrostatic map: the black and grey polyhedra describe regions where a high electron density within the ligand structure increases or decreases, respectively, the affinity for the adenosine A<sub>1</sub> receptor (model 14, Table 7).

Table 6. Non-leave-one-out cross-validation of the best obtained CoMFA models

Samples	Number of omitted compounds	$q^2$ of model 9 'N6-C8' alignment rule	$q^2$ of model 12 'N6-N7' alignment rule
5	9	0.7645	0.7797
6	8	0.7203	0.7403
7	7	0.6917	0.7009
8	6	0.7411	0.7384
9	5	0.6949	0.7195
Mean $q^2$		0.7225	0.7358
$q^2$ of leave-one-out cv		0.7253	0.7828
Non-cross-validated $r^2$		0.8251	0.8653

Table 7. Statistics of the 'N6-N7' CoMFA model

CoMFA model	$n$	PC <sup>a</sup>	$q^2$	$e_{\text{PRESS}}$	$r^2$
Model 12					
steric + electrostatic	45	2	0.7828	0.4560	0.8653
Model 13					
only steric	45	3	0.6698	0.5613	0.8058
Model 14					
only electrostatic	45	3	0.6129	0.6077	0.6988

<sup>a</sup>Number of principal components explaining more than 80% of total variance.

to the A<sub>1</sub> adenosine receptors is modulated by steric and electrostatic factors simultaneously.

(b) All the 'N6-N7' CoMFA models provide slightly better predictions than the 'N6-C8' ones. In the 'N6-C8' model the electrostatic overlap between xanthenes and adenosines is better than the steric one (Table 5, models 10 and 11). Conversely, the steric correspondence of xanthenes and adenosines is better than the electrostatic one in the 'N6-N7' model (Table 7, models 13 and 14). However, both steric and electrostatic superpositions in the 'N6-N7' model are slightly better than in 'N6-C8'.

(c) There is only one difference between the coefficient maps created according to the two models. This is the steric restriction around the N6-H in the 'N6-N7' steric field map, which is absent in the 'N6-C8' steric field map.

The 'N6-N7' model does not contradict the 'N6-C8' model. It is a variance of 'N6-C8' with more precise steric and electrostatic overlaps of adenosine agonists and xanthine antagonists. Thus, all the evidence supporting the 'N6-C8' model is also valid for the 'N6-N7' model. For example, the stereoselectivity in the binding of N6-phenylisopropyladenosine and 8-phenylisopropylxanthine to the A<sub>1</sub> adenosine receptors (*R*-enantiomers are more active than *S*-enantiomers) is one of the most important pieces of

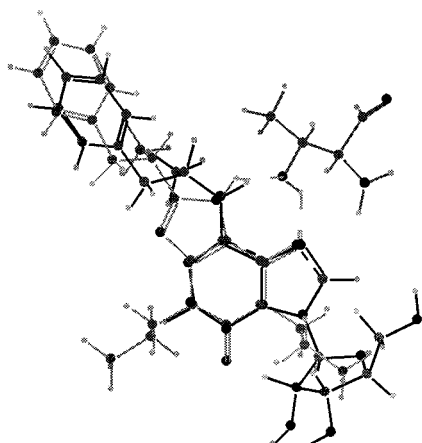


Figure 7. Alignment of *R*-1,3-dipropyl-8-phenylisopropylxanthine (grey contour) on **R-PIA** (black contour). H-bonds (grey interrupted contours) with the OH group of Thr 277 (black contour upper right) are shown. N6/N7 atoms act as H-bond donors. N7/O6 atoms act as H-bond acceptors.

evidence for the 'N6-C8' model [3]. The 'N6-N7' mode of binding confirms this (Figure 7).

Further evidence for the 'N6-C8' model is the finding that 9-deazaxanthines are as potent as or more potent than the corresponding xanthines at A<sub>1</sub> adenosine receptors, while the 7-deazaxanthines are less potent [24]. The 'N6-N7' mode of binding fully agrees with this finding as the N6 of adenosines superimposes precisely the N7 of xanthines (Figure 1d).

A very reliable hypothesis exists that N6 from adenosine acts as a hydrogen bond donor with His 251 [25] or with Thr 277 [26] of the A<sub>1</sub> receptor (Figure 7). At a certain distance from N6 the atom N7 acts as a hydrogen bond acceptor with Thr 277 [26]. In the xanthines, atoms N7 (hydrogen bond donor) and O6 (hydrogen bond acceptor) play these roles. According to the 'N6-C8' model the distance between N6 of adenosines and N7 of xanthines is 0.947 Å and the distance between N7 of adenosines and O6 of xanthines 0.960 Å [5]. According to the 'N6-N7' model the same distances are only 0.101 Å and 0.215 Å, respectively [5].

## Conclusions

The CoMFA method has been successfully applied to compare two models of the binding site of adenosine A<sub>1</sub> receptors. The resulting 3D-QSAR models provide significant correlation of steric and electrostatic fields with the affinity constants of adenosine ago-

nists and xanthine antagonists. The 'N6-N7' mode of binding produces slightly better predictions in comparison with the 'N6-C8' model. Without rejecting the 'N6-C8' model, 'N6-N7' is a further development with better steric and electrostatic overlaps between agonists and antagonists.

## Acknowledgements

The author thanks Sonja Meddeb of Chemical Design Ltd., France, for help in the use of Chem-X software, Dr Ilsa Pajeva, Bulgarian Academy of Sciences, for the helpful discussion, and Dr Nikolay Todorov, Drug Design Group, University of Cambridge, for the English cross-check. This work was supported by a grant from the Medical Science Research Council at the Medical University, Sofia, Bulgaria.

## References

- Libert, F., Schiftmann, S.N., Lefort, A., Partmentier, M., Gerard, C., Dumont, J.E., Vanderhaeghen, J.-J. and Vassart, G., *EMBO J.*, 10 (1991) 1677.
- van Galen, P.J.M., van Vlijmen, H.W.Th., IJzerman, A.P. and Soudijn, W., *J. Med. Chem.*, 33 (1990) 1708.
- Peet, N.P., Lentz, N.L., Meng, E.C., Dudley, M.V., Ogden, A.M.L., Demeter, D.A., Weintraub, H.J.R. and Bey, P., *J. Med. Chem.*, 33 (1990) 3127.
- van der Wenden, E.M., IJzerman, A.P. and Soudijn, W., *J. Med. Chem.*, 35 (1992) 629.
- Doytchinova, I. and Petrova, S., *Med. Chem. Res.*, 8 (1998) 143.
- Pajeva, I. and Wiese, M., *J. Med. Chem.*, 41 (1998) 1815.
- Sadler, B.R., Cho, S.J., Ishaq, K.S., Chae, K. and Korach, K.S., *J. Med. Chem.*, 41 (1998) 2261.
- Mor, M., Rivava, S., Silva, C., Bordi, F. and Plazzi, V., *J. Med. Chem.*, 41 (1998) 3831.
- Trivedi, B.K. and Bruns, R.F., *J. Med. Chem.*, 32 (1989) 1667.
- Jacobson, K.A., van Galen, P.J.M. and Williams, M., *J. Med. Chem.*, 35 (1992) 407.
- Trivedi, B.K., Blankley, C.J., Bristol, J.A., Hamilton, H.W., Patt, W.C., Kramer, W.J., Johnson, S.A., Bruns, R.F., Cohen, D.M. and Ryan, M.J., *J. Med. Chem.*, 34 (1991) 1043.
- Shamim, M.T., Ukena, D., Padgett, W.L. and Daly, J.W., *J. Med. Chem.*, 32 (1989) 1231.
- Shamim, M.T., Ukena, D., Padgett, W.L., Hong, O. and Daly, J.W., *J. Med. Chem.*, 31 (1988) 613.
- van der Wenden, E.M., van Galen, P.J.M., IJzerman, A.P. and Soudijn, W., *J. Med. Str. (Theochem)*, 231 (1991) 175.
- Chem-X (July 1998. Chemical Design Ltd., Chipping Norton, Oxfordshire OX7 5SR, U.K.
- Burkert, U. and Allinger, N.L., *Molecular Mechanics*, Am. Chem. Soc., Washington, DC, 1982.
- Dewar, M.J.S., Zoebisch, E.G., Healy, E.F. and Stewart, J.J.P., *J. Am. Chem. Soc.*, 107 (1985) 3902.
- Dunn, W.J., III, Wold, S., Edlund, U., Hellberg, S. and Gasteiger, J., *Quant. Struct. - Act. Relat.*, 3 (1984) 131.

19. Wold, S., In Van de Waterbeemd, H. (Ed.) *Chemometric Methods in Molecular Design*, VCH, Weinheim, 1995, pp 195–218.
20. Mueller, Chr., *Exp. Opin. Ther. Patents*, 7 (1997) 419.
21. Bruns, R.F., Lu, G.H. and Pugsley, T.A., *Mol. Pharmacol.*, 29 (1986) 331.
22. Lohse, M.J., Klotz, K.-N., Schwabe, U., Cristalli, G., Vitori, S. and Grifantini, M., *Naunyn-Schmiedeberg's Arch. Pharmacol.*, 29 (1988) 687.
23. Nair, V. and Fasbender, A.J., *Tetrahedron*, 49 (1993) 2169.
24. Grahner, B., Winiwarter, S., Lanzner, W. and Muller, C.E., *J. Med. Chem.*, 37 (1994) 1526.
25. IJzerman, A.P., van Galen, P.J.M. and Jacobson, K.A., *Drug Des. Discov.*, 9 (1992) 49.
26. Dudley, M.W., Peet, N.P., Demeter, D.A., Weintraub, H.J.R., IJzerman, A.P., Nordvall, G., van Galen, P.J.M. and Jacobson, K.A., *Drug Dev. Res.*, 28 (1993) 237.